Asian Journal of Chemistry; Vol. 31, No. 3 (2019), 733-743

ASIAN JOURNAL OF CHEMISTRY

https://doi.org/10.14233/ajchem.2019.21515

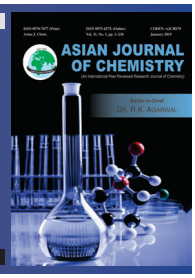

Spectral and Thermal Studies of Some Nucleic Acid Complexes

MAMDOUH S. MASOUD, MAGDA F. FATHALLA*, RABAH HANEM A. MOHAMED and MAISA S. HASSAN

Chemistry Department, Faculty of Science, Alexandria University, P.O. 426 Ibrahimia, Alexandria 21321, Egypt

*Corresponding author: E-mail: mffathalla@hotmail.com

Received: 20 August 2018; *Accepted*: 30 December 2018; *Published online*: 31 January 2019; AJC-19278

Barbituric acid, thiobarbituric acid and thiouracil complexes with sodium and potassium chlorides were prepared and characterized by UV in different solvents and IR experimentally and theoretically using B3LYP method and Gaussian program. The composition of the studied complexes was also confirmed by elemental and thermal analysis, TG, DTA and DSC techniques to determine thermodynamic parameters (E_a, ΔH, ΔS and ΔG). The negative value of entropy of activation indicated the fragments have ordered structures than undecomposed complexes. The positive values of enthalpy of activation of the decomposition stages indicated that the process is endothermic. The positive values of free energy of the decomposition indicated non-spontaneous process. Evaluation of kinetics parameters were done. The isokinetic temperature β is 407 K, which is lower than experimental temperature range, confirming the processes is entropy control. However, the plots of ΔH *versus* ΔS for the complexes under investigation gave straight line indicating a close similarity in the mechanism.

Keywords: Nucleic acid, Complexes, Spectral, Thermal.

INTRODUCTION

Barbituric acid always attracts attention because of great importance for biology and medicinal applications [1,2] as anticonvulsants, narcotics, soporifics, sedative hypnotics, anxyiolytics and tranquilizer [3,4]. Thiobarbituric acid derivatives have vast medicinal importance showing a number of activities *e.g.* antifungal [5] antidepressant [6], antimicrobial [7], antitubercular, antiherbicides [8], antioxidant, membrane protector [9] and radio protector [10]. 2-Thiouracil (2-mercapto-4-hydroxypyrimidine) (2TU) is a thio-derivative of uracil, one of the nucleic acid bases (NABs). Its biological importance had been established as an antithyroid drug [11], antiviral agent [12] and anticarcinogenic agent [13-15].

Aim of the work is focused to synthesize barbaturic, thiobarbaturic and uracil complexes with NaCl and KCl to examine the effect of molecular structure on their UV-visible spectra. A careful analysis of the obtained data using statistical techniques showed that the solvatochromism correlate to the identity of the complexes and the solvent parameters. Infrared spectra for the complexes were carried out using experimental and theoretical studies using Gaussian program [16]. The composition of the studied complexes was confirmed by thermal analysis (TG, DTA and DSC). The thermodynamic parameters are evaluated and discussed.

EXPERIMENTAL

Synthesis of the complexes: Complexes **I, II** (structures 2,3) were prepared by dissolving 0.128 g of barbituric acid (structure 1) in 10 mL distilled water followed by adding 0.075 g of potassium chloride in case of preparation of complex **I** and 0.224 g in case of complex **II**. The solution mixtures were heated for a few minutes until the volume of solution decreased to the half and the precipitated complexes were formed and then dried. The complex **III** (structure 5) was prepared by dissolving 0.1442 g of thiobarbituric acid (structure 4) in 10 mL distilled water then 0.058 g of sodium chloride was added. The complex **IV** (structure 7) (TU.3KCl) was prepared by dissolving 0.128 g of thiouracil (structure 6) in 10 mL distilled water followed by adding 0.075 g of potassium chloride. The physico-analytical data of the complexes are given in Table-1.

Spectral measurements: FTIR of the ligands and their complexes were taken in potassium bromide disc using Perkin Elmer spectrophotometer, Model 1430 covering frequency range 4000-200 cm^{-1}. The electronic spectra of complexes under investigation in presence of eight solvents (ethanol,

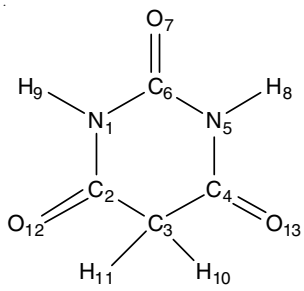

Structure **1** Barbituric acid (BA)

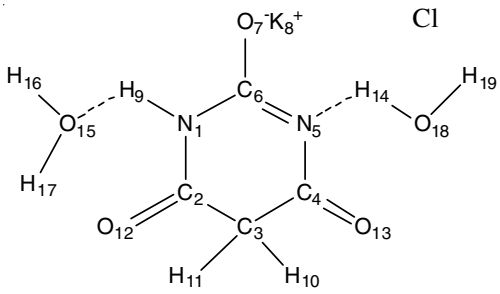

Structure **2** complex (**I**)

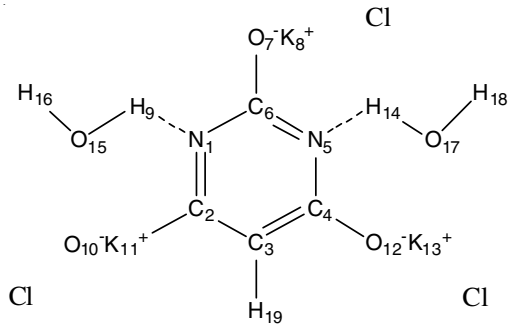

Structure **3**: complex(**II**)

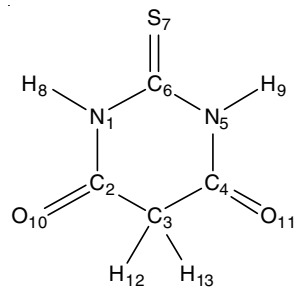

Structure **4** (SBA)

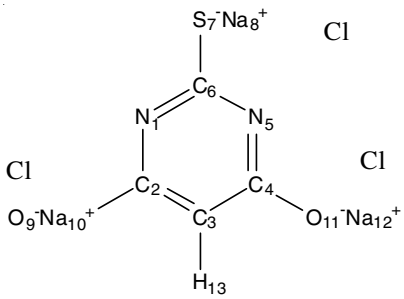

Structure **5**, complex (**III**)

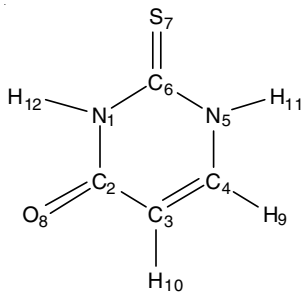

Structure **6** thiouracil

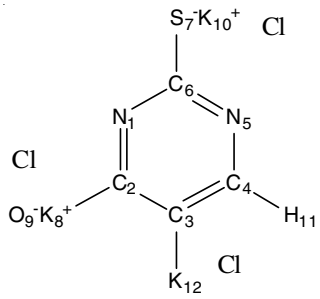

Structure **7**, complex (**IV**)

TABLE-1
PHYSICO-ANALYTICAL DATA FOR THE COMPLEXES

Complex	Colour	m.f.	Elemental analysis (%): Calcd. (Found)			
			C	H	N	Cl
BA.KCl.2H_2O (**I**)	Pale orange	$C_4H_4N_2O_3KCl{\cdot}2H_2O$	20.13 (20.12)	1.68 (1.51)	11.74 (11.75)	14.88 (14.56)
BA.3KCl.2H_2O (**II**)	Light brown	$C_4H_4N_2O_3{\cdot}3KCl{\cdot}2H_2O$	12.38 (12.45)	1.03 (2.42)	7.22 (7.72)	27.47 (27.82)
SBA.3NaCl (**III**)	Pale pink	$C_4H_4N_2SO_2{\cdot}3NaCl$	15.02 (15.32)	1.25 (1.35)	8.76 (9.32)	33.34 (32.42)
Tu.3KCl (**IV**)	Yellowish white	$C_4H_4N_2SO{\cdot}3KCl$	13.65 (14.11)	1.14 (1.46)	7.96 (8.44)	30.29 (29.13)

methanol, acetonitrile, dimethylformamide, dimethysulfoxide chloroform, dioxane and water) were obtained using recording JascoV-530 UV/visible spectrophotometers. The spectral data were analyzed by the multiple linear regression technique using statistical package of social science program, SPSS version 15 and the calculations have been carried out on a personal computer to obtain the different statistical parameters. The Gaussian computer program [16] has been used to calculate the theoretical infrared spectra of complexes. Thermal analysis (DTG, TGA and DSC) were carried under nitrogen atmosphere under heating rate 10 °C/min, Faculty of Science, Cairo University.

RESULTS AND DISCUSSION

Solvent effects on the electronic absorption spectra: The absorption spectra of the investigated complexes in the UV region are highly affected either position or intensity [17-22]. The change in λ_{max} is taken as a standard to solvent effects (Table-2). The solvent polarizability effect, leads to red shift due to the stabilization of the excited state by the induced dipole interaction between the transition dipole of solute and the solvent molecules [23].

Methods of calculations

Data analysis: The observed peak position of an absorption band λ_{max} in a given solvent as the dependent variable Y may be expressed as a function of different solvent polarity parameters x_n as follows:

$$Y = a_o + a_1x_1 + a_2 x_2 + a_3 x_3 + \ldots\ldots + a_nx_n \quad (1)$$

Eqn. 1 is amenable to solution for the intercept a_o and the coefficients a_1, a_2, a_3, ...+ a_n by multiple regression

TABLE-2
EFFECT OF SOLVENTS ON THE ELECTRONIC ABSORPTION SPECTRA OF THE COMPLEXES

Solvent	λ_1				λ_2				λ_3				λ_4			
	I	II	III	IV	I	II	III	IV	I	II	III	IV	I	II	III	IV
Dioxane	–	258	245	–	256	–	–	270	–	285	294	–	–	–	–	–
$CHCl_3$	–	264	232	231	232	277	–	271	282	–	283	291	–	–	–	–
Ethanol	215	258	212	214	255	–	–	–	–	283	291	–	–	–	–	–
Methanol	215	258	234	213	255	315	–	272	329	283	293	–	328	–	–	–
DMF	268	–	–	–	268	315	271	272	328	285	295	–	–	–	–	–
Acetonitrile	207	254	233	210	254	–	–	268	–	282	290	–	–	–	–	–
DMSO	–	264	–	–	264	316	265	270	317	328	288	297	329	–	–	–
H_2O	–	254	242	212	–	318	262	270	314	326	280	–	328	–	–	–

technique. The regression intercept a_o has been considered as a peak position in the gas phase. One, two and three parameters equations are applied using suitable combination between the solvent polarity parameters E, K, M, J, H and N as reported before [23]. The dielectric function K represents the dipolar interaction [24].

$$K = (D-1)/(2D+1) \quad (2)$$

where D is the dielectric constant. The parameter E is sensitive to both solute-solvent hydrogen bonding and dipolar interaction:

$$E = 2.859 \times 10^{-3} \nu^{-} \quad (3)$$

ν^{-} is the wave number of the absorption maximum in a given solvent [24].

The functions H and J have been introduced to account for the non-specific solute- solvent interactions such as dispersion and dipolar effects.

$$J = (D-1)/(D+1),\ H = (n^2 - 1)/(n^2 + 2) \quad (4)$$

where n is the solvent refractive index. The parameters N and M are the measure of the permanent dipole-solvent induced dipole and solute permanent dipole-solvent permanent dipole interactions respectively $M = (n^2-1)/(2n^2 + 1)$, N = J–H [25-29]. The values of solvent parameters E, M, N, K, D, n, X_1 and X_2 in different solvents are given in Table-3. The solvent induced spectral shifts observed for the prepared complexes (**I-IV**) have been analyzed using the multiple linear regression technique (SPSS program). In each case fits are obtained as a function of parameter E, M, N and K, each of which alone then obtained as two parameters (E, M), (E, N), (E, K), (M, N), (M, K) and (N, K), the three parameters (E, M, N), (E, M, K), (E, N, K) and (M, N, K) and four parameters (E, M, N, K) for the complexes at different wavelengths [30] are given in Tables 4-7.

TABLE-3
SOLVENT PARAMETERS, X_1 AND X_2 FOR SOLVENTS

Solvent	D	N	E	M	N	K	X_1	X_2
Dioxane	2.20	1.422	36.0	0.20	0.03	0.22	0.4444	0.4300
Chloroform	4.70	1.446	39.1	0.21	0.29	0.36	0.7115	0.4191
Ethanol	24.3	1.361	51.9	0.18	0.67	0.47	0.9395	0.3623
Methanol	32.6	1.329	55.5	0.17	0.71	0.48	0.9546	0.3381
DMF	36.7	1.427	43.8	0.20	0.67	0.48	0.9597	0.4086
Acetonitrile	37.5	1.346	46.0	0.18	0.71	0.48	0.9605	0.3496
DMSO	48.9	1.478	45.0	0.22	0.66	0.48	0.9696	0.4412
H_2O	78.5	1.333	63.1	0.17	0.76	0.49	0.9810	0.3442

$X_1 = 2(D-1)/(2D+1)$ $X_2 = 2(n^2-1)/(2n^2+1)$

TABLE-4
REGRESSION ANALYSIS FOR COMPLEX **I** (BA·KCl·$2H_2O$) IN DIFFERENT SOLVENTS AT λ_3

Parameters	a_0	a_1	a_2	a_3	a_4	MCC	P
E	38409.79	-111.240	–	–	–	0.408	0.559
M	28647.22	21522.0	–	–	–	0.068	0.832
N	37781.82	-8474.03	–	–	–	0.928	–
K	46174.08	-29825.1	–	–	–	0.981	0.088
E, M	83328.96	-404.850	-152563.5	–	–	1	–
E, N	35691.78	82.294	-11891.31	–	–	1	–
E, K	46442.24	35.584	-34368.3	–	–	1	–
M, N	43739.20	-25772.8	-9882.492	–	–	1	–
M, K	49422.44	-12326.1	-31591.57	–	–	1	–
N, K	54632.08	9058.95	-60550.52	–	–	1	–

TABLE-5
REGRESSION ANALYSIS FOR COMPLEX **II** (BA·3KCl·$2H_2O$) IN DIFFERENT SOLVENTS AT λ_2

Parameters	a_0	a_1	a_2	a_3	a_4	MCC	P
E	38753.16	-126.087	–	–	–	0.381	0.268
M	25741.87	35026.70	–	–	–	0.163	0.500
N	39017.54	-10486.23	–	–	–	0.971	0.002
K	49165.66	-36307.01	–	–	–	0.999	0.000
E, M	53811.33	-231.197	-50908.68	–	–	0.461	0.539
E, N	37753.40	49.499	-12389.44	–	–	0.997	0.003
E, K	49179.27	5.821	-36963.27	–	–	1.000	0.000
M, N	42977.17	-16809.60	-11616.59	–	–	0.997	0.003
M, K	49828.68	-2403.164	-36736.72	–	–	1.000	0.000
N, K	50827.64	1790.675	-42352.02	–	–	1.000	0.000
E, M, N	40377.92	27.982	-8808.89	-12154.5	–	0.999	0.029
E, M, K	49800.31	0.337	-2297.49	-36755.8	–	1.000	0.020
E, N, K	53982.16	-12.748	5221.59	-52496.9	–	1.000	0.016
M, N, K	50187.66	-1633.276	615.628	-38677.3	–	1.000	0.019

TABLE-6
REGRESSION ANALYSIS FOR COMPLEX **III** (SBA:3NaCl) IN DIFFERENT SOLVENTS AT λ_2

Parameters	a_0	a_1	a_2	a_3	a_4	MCC	P
M	39822.8	-1129526	–	–	–	0.195	0.709
N	31900.4	8183.269	–	–	–	0.699	0.507
K	-3473.7	84983.00	–	–	–	0.580	0.449
E, M	24746.5	119.469	34605.88	–	–	1.000	0.000
E, N	56620.7	291.923	-48517.21	–	–	1.000	0.000
E, K	590553	696.233	-1216973	–	–	1.000	0.000
M, N	2665.46	58579.27	33610.53	–	–	1.000	0.000
M, K	-92452.4	41774.00	252079	–	–	1.000	0.000
N, K	-328893	-83548	878689	–	–	1.000	0.000

TABLE-7
REGRESSION ANALYSIS FOR COMPLEX **IV** (Tu:3KCl) IN DIFFERENT SOLVENTS AT λ_1

Parameters	a_0	a_1	a_2	a_3	a_4	MCC	P
M	64213.0	-98141.6	–	–	–	0.856	0.024
N	40743.7	8929.23	–	–	–	0.964	0.003
K	31887.1	31719.6	–	–	–	0.971	0.002
E, M	78977.6	-105.872	-149528.5	–	–	0.930	0.070
E, N	42363.7	-59.762	11214.34	–	–	0.999	0.001
E, K	31427.2	-49.151	38238.29	–	–	0.996	0.004
M, N	24656.2	68602	14664.74	–	–	0.985	0.015
M, K	11566.0	64181.2	50667.74	–	–	0.991	0.009
N, K	15428.1	-16707.6	90823.44	–	–	0.976	0.024
E, M, N	38942.4	-53.413	13855.49	12129.96	–	1.000	0.027
E, M, K	24653.5	-38.055	43179.39	21721.58	–	0.997	0.068
E, N, K	51824.2	-68.338	20887.36	-33106.89	–	1.000	0.010
M, N, K	7465.22	60523.8	-5338.23	68471.72	–	0.991	0.121
E, M, N, K	48784.4	-64.145	6131.39	19732.55	-27767.7	1.000	0.000

The multiple correlation coefficient (MCC) has been used in one-tail test to obtain the level of significance for each test. This value is considered as a measure of the goodness of the fit. The high value of MCC (near one) means that a certain solvent parameter has a good correlation to the spectral shift. The spectral shifts for the peak are greatly sensitive to the solvent parameter that gives a value of MCC near to unity. Alternatively, the small values (near zero) of the significance parameter (P) mean the correlation is good. The parameters that gave the best correlation and best significance among the other for the different electronic transitions of the investigated compounds (Tables 4-7), indicating that all solvent parameters are sensitive to dipolar and hydrogen bonding interaction, other interaction such as dispersion force, solvent induced dipole and solute permanent dipole-solvent permanent interaction.

The values of the multiple correlation coefficient indicated that experimental data are best fitted in case of one-parameter equation, the parameter (K) plays the important role for determining the spectral shifts for complex **I** at λ_3, for complex **II** at λ_2 and for complex **IV** at λ_1 (Tables 4-7). The relative high value of the multiple regression coefficient and the lower value of the probability of variation (P) for the parameter (K) points to that the solute permanent dipole-solvent induced dipole interactions are playing the important role to explain the spectral shifts observed. However, the parameter (N) is important for determining the spectral shifts for complex **I**, **II** and **IV**. The relative high value of the multiple regression coefficients for parameter (N) points to that the dielectric constant is effective to explain the spectral shifts rather than the electronic character of the substituents. The parameter (M) is important for determining the spectral shifts for complex **IV** at λ_1, the relative high value of multiple regression coefficient and the lower value of the probability of variation (P) for the parameter (M) point to that the solute permanent dipole-solvent induced dipole interactions are playing the important role to explain the spectral shifts observed. For the two parameters equation, the combination (E, M), (E, N), (E, K), (M, N), (M, K) and (N, K) give higher values of correlation for complex **I** at λ_3, complex **II** at λ_2, complex **III** at λ_2 and complex **IV** at λ_1, due to high value of the multiple regression coefficients and the lower value of the probability of variation (P). So, the solute permanent dipole solvent induced dipole combined with solute permanent dipole-solvent permanent dipole interactions are major factors for determining the spectral shifts. For three parameters equation, the combination (M, N, K), (E, M, N), (E, M, K) and (E, N, K) give high values of correlations for complex **II** and **IV** as shown by its multiple regression coefficient and low probability of variation (P). So, the intermolecular hydrogen bonding combined with solute permanent dipole-solvent induced dipole and solute permanent dipole-solvent permanent dipole interactions are effective parameters to explain the spectral shifts. So, the effect the intermolecular hydrogen bonding is of major effect. The addition of four solvent parameter to the three parameter equations give rise to improvements in the correlation with the solvent induced spectral shifts. For the parameters (E, M, N, K) give high value of correlation complex **IV** at λ_1.

The spectra for each solvent are correlated with physical properties of solvents especially the dielectric constant, D and the refractive index (n). K_1, K_2, ν_{vapour}, MCC and P are computed (Table-8). The data showed that the dielectric constant D and

TABLE-8
K_1, K_2, ν_{vapour} AND CORRELATION ANALYSIS FOR THE COMPLEXES

Complex	ν_{vapour} (cm^{-1})	K_1	K_2	MCC	P
I (λ_1)	-113722.3	137473.4	85778.861	1.000	0.000
I (λ_2)	47531.462	-4553.209	-11100.969	0.186	0.662
I (λ_3)	47981.530	-14752.01	-4830.546	1.000	0.000
I (λ_4)	30597.103	214.887	-930.003	1.000	0.000
II (λ_1)	46682.648	-1852.511	-16989.46	0.668	0.064
II (λ_2)	48110.181	-17337.67	757.712	0.999	0.001
II (λ_3)	24372.450	5972.800	1149.819	0.971	0.172
III (λ_1)	3465.297	16442.135	69184.992	0.359	0.513
III (λ_2)	-33251.35	71420.405	3939.202	1.000	0.000
III (λ_3)	38372.749	-523.155	-6880.260	0.729	0.038
IV (λ_1)	30508.121	16243.217	2953.783	0.973	0.027
IV (λ_2)	37383.815	-115.913	-783.306	0.025	0.950
IV (λ_3)	36973.337	-620.916	-5894.114	0.541	0.211

the refractive index (n) of solvents affect on the electronic absorption spectra [27,28]. The ν_{vapour} values and the coefficients K_1 and K_2 were determined, based on linear regression, the function $\nu_{solution}$ is linear in both D and n, eqn. 6 is applied. Table-8 explains the solvent parameter relation for the complexes (**I-IV**) with different solvents as follows:

$$\nu_{solution} = \nu_{vapour} + K_1[2(D-1)/2D+1] + K_2[2(n^2-1)/2n^2+1] \quad (5)$$

$$\nu_{solution} = \nu_{vapour} + K_1X_1 + K_2X_1 \quad (6)$$

• The best correlation for complex **I** ($BA{\cdot}KCl{\cdot}2H_2O$) is at λ_3 and for complex **II** ($BA{\cdot}3KCl{\cdot}2H_2O$), the best correlation is at λ_2. However complex **III** (SBA: 3NaCl) is at λ_2 while for complex **IV** (Tu: 3KCl) at λ_1 where the value of MCC near to unity.

• The K_1 value (which is related to dielectric constant of the solvents) of complex **I** is higher due to the polarity of the solvent which affected on the investigated complexes.

• The negative charge of K_2 values (related to the refractive index of the solvents) means that the forces of the solute-solvent interactions are in the same direction, while the positive charge of K_2 values are of the opposite trend.

Table-9 shows the solvent parameter relation for the complexes and Fig. 1 for the plot of $K_1X_1 + K_2X_2$ *versus* ν (cm^{-1}).

Multi parameter analysis: The effects of solvent polarity and hydrogen bonding on absorption spectra are interpreted by means of the linear solvation energy relation energy (LSER) concept [27], using general solvatochromic of the following form:

$$\nu_{max} = \nu_o + a\,\alpha + b\,\beta + s\,\pi^* \quad (7)$$

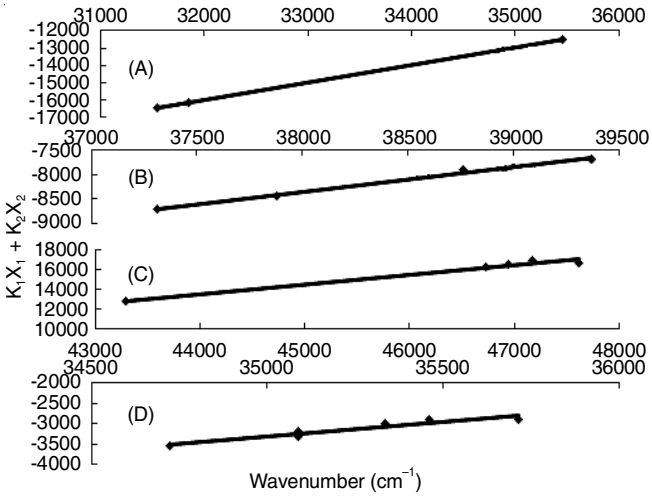

Fig. 1. Solvent parameter-relation for (A) $BA{\cdot}KCl{\cdot}2H_2O$, (B) $BA{\cdot}3KCl{\cdot}2H_2O$, (C) Tu:3KCl, (D) SBA:3NaCl

where α, β and π^* are solvatochromic parameters and (s), (a) and (b) are solvatochromic coefficients. π^* is an index of dipolarity/polarizability, which a measure of the ability of the solvent to stabilize a charge or dipole by its own dielectric effects [29].

The multiple linear regression correlate electronic spectra data ν_{max} with the solvatochromic parameters [25] α, β and π^* for protic, non-polar and dipolar aprotic solvents.

For complex I ($BA{\cdot}KCl{\cdot}2H_2O$):

$$\nu_{max} = (52057.9 \pm 2291.3) - (3900 \pm 1122)\,\alpha - (2352 \pm 1697)\beta - (13739 \pm 2365)\pi^* \quad (8)$$

$$(n = 7,\ s = 1249,\ F = 13.65,\ r = 0.97)$$

TABLE-9
SOLVENT PARAMETER-RELATION FOR THE COMPLEXES

ν (cm^{-1})				$K_1X_1 + K_2X_2$			
Complex **I**	Complex **II**	Complex **III**	Complex **IV**	Complex **I**	Complex **II**	Complex **III**	Complex **IV**
–	38759.69	35087.72	–	-8632.92	-8128.73	-3191	8488.62
35460.99	37878.79	35335.69	43290.04	-12520.54	-8438.35	-3255.744	12794.98
–	38759.69	35335.69	46728.97	-15609.62	-7895.71	-2984.224	16330.66
–	38759.69	35335.69	46948.36	-15715.48	-7512.55	-2825.624	16504.44
–	37313.43	35087.72	–	-16131.26	-8719.74	-3313.34	16795.54
–	39370.08	35460.99	47619.05	-15858.07	-7687.04	-2907.83	16634.25
31545.74	37878.79	34722.22	–	-16434.79	-9291.95	-3542.82	17052.63
31847.13	39370.08	35714.29	47169.81	-16134.39	-7665.08	-2881.41	16951.29

For complex II (BA·3KCl·2H$_2$O):

$$\nu_{max} = (57101 \pm 4916) - (1271 \pm 1569)\,\alpha - (7945 \pm 3516)\beta - (20669 \pm 3764)\,\pi^* \quad (9)$$

β and π* parameters are the most effective, the α parameter is neglected, so

$$\nu_{max} = (57101 \pm 4916) - (7945 \pm 3516)\beta - (20669 \pm 3764)\,\pi^* \quad (10)$$

n = 6, s = 1533, F = 10.8, r = 0.97

For complex III (SBA·3NaCl):

$$\nu_{max} = (333708 \pm 727) + (1433 \pm 387)\,\alpha - (1446 \pm 634)\beta + (2523 \pm 832)\pi^* \quad (11)$$

n = 8, s =478, F = 10.5, r = 0.97

For complex IV (TU.3KCl):

$$\nu_{max} = (32805 \pm 726.9) + (1392 \pm 387)\,\alpha - (1547 \pm 634)\beta + (2385 \pm 831)\,\pi^* \quad (12)$$

n = 8, s = 477, F= 10.2, r = 0.94

where n is the number of solvents, s is the standard deviation, F is statistic and r is the correction coefficient.

For complex **I**, α, β and π* parameters are the most effective parameters on the absorption wavenumber, the hydrogen bond donor and acceptor and polarity-dipolarizability. For complex **II**, β and π* parameters are the most effective parameters, while for complex **III** and complex **IV**, α, β and π* parameters are effective. The electronic absorption spectral data (ν_{max}) is in correlation with solvatochromic parameters α, β and π* for protic and aprotic solvents. The results of correlation with solvatochromic parameters (α, β and π*) and the coefficients a, b and s from eqn. 7 are given in eqns. 8-12. Percentage contributions based on eqns. 8-12 for different organic solvents are shown in Fig. 2.

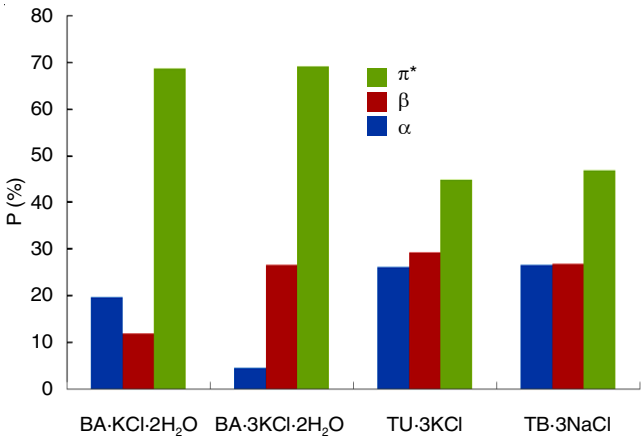

Fig. 2. Percentage contribution P (%) to the solvatochromic effects

Smoothly, the systematic multiple regression analysis leads to the following:

• For all complexes (**I-IV**), the contribution of the solvent dipolarity/polarizability to the total effect is predominant.

TABLE-10
FUNDAMENTAL INFRARED FREQUENCIES (cm^{-1}) OF THE LIGANDS AND THEIR COMPLEXES (**I-IV**)

Compound	ν(NH)	ν(OH)	ν(CH$_2$) & ν(CH)	ν(C=O) & ν(C-O)	ν(C=C) & ν(C-C)	ν(C=N) & ν(C-N)	ν(C=S) & ν(C-S)
BA	3561, 3477	-	3100	1749, 1717	1619	1193	-
BA·KCl·2H$_2$O (**I**)	3558, 3476	3186	3186, 3101	1747, 1717	1619	1528 & 1192	-
BA·3KCl·2H$_2$O (**II**)	3474	3182	-	1708	1619, 1585	1473 & 1193	-
SBA	3563	-	3104	1693	1607	1442	1163
SBA·3NaCl (**III**)	-	-	3102	1717	1572	1438	1164
Tu	3465	-	3084	1706	1625	1425	1166
Tu.3KCl (**IV**)	-	-	3083	1702	1562	1421	1165

TABLE-11
THEORETICAL AND EXPERIMENTAL INFRARED SPECTRA OF BARBITURIC ACID AND ITS COMPLEXES

BA			BA.KCl.2H$_2$O			BA.3KCl.2H$_2$O		
Gaussian	Experimental	Assignment (cm^{-1})	Gaussian	Experimental	Assignment (cm^{-1})	Gaussian	Experimental	Assignment (cm^{-1})
3615	3562	ν(N$_1$-H$_9$), ν(N$_5$-H$_8$)	3877	3186	ν(O$_{15}$-H$_{16}$), ν(O$_{15}$-H$_{17}$)	3725	3182	ν(O$_{15}$-H$_9$), ν(O$_{15}$-H$_{16}$), ν(O$_{17}$-H$_{14}$), ν(O$_{17}$-H$_{14}$)
3118	3187	ν(C$_3$H$_{10}$H$_{11}$) asym	3663	3558	ν(N$_1$-H$_9$)	–	3474	ν(N$_1$-H$_9$)
3082	3100	ν(C$_3$H$_{10}$H$_{11}$) sym	3332	3186	ν(C $_3$H$_{10}$H$_{11}$) asym.	3041	–	ν(C $_3$-H$_9$)
–	1619	ν(C$_2$-C$_3$), ν(C$_3$-C$_4$)	3280	3101	ν(C$_3$H$_{10}$H$_{11}$)sym.	1543	1585	ν(C$_2$-C$_3$), ν(C$_3$=C$_4$)
1235	1193	ν(C$_4$-N$_5$), ν(C$_2$-N$_1$)	1673	1619	ν(C$_2$-C$_3$), ν(C$_3$-C$_4$)	1116, 1449	1193, 1473	ν(C$_6$=N$_5$), ν(C$_6$-N$_1$)
1820	1750	ν(C$_2$=O$_{12}$), ν(C$_4$=O$_{13}$), ν(C$_6$=O$_7$)	1511	1528	ν(C$_4$-N$_5$), ν(C$_2$-N$_1$)	824		ν(C $_2$-O$_{10}^-$), ν(C$_4$-O$_{12}^-$), ν(C$_6$-O$_7^-$)
			–	1717-1747	ν(C$_2$=O$_{12}$), ν(C$_4$=O$_{13}$)			

• The positive sign of the (s) parameter indicates that the value of this parameter increases with increasing polarity of solvent and negative values of (s) for complexes **I** and **II** show a positive solvatochromism of the studied complex with solvents dipolarity/polarizability. This suggests a higher stabilization of the electronic excited state as compared to the ground state stabilization.

• The negative sign of (b) coefficient indicates that the decrease in hydrogen bond acceptor formation.

• The positive values of (a) coefficient for complexes **III** and **IV** lead to the increase of hydrogen bond donor ability, while for **I** and **II** leading to the decrease of hydrogen bond donor ability with the solvent.

The percentage contribution of solute-solvent, dipole-dipole interaction π^* dipolarity/polarizability (non-specific solute-solvent interaction) is much morepronounced than the specific ones (α and β, Fig. 2) for all selected complexes.

Infrared spectra: The fundamental frequencies of barbituric acid, thiobarbituric acid, thiouracil and their complexes (**I**-**IV**) are given in Table-10.

Theoretical infrared spectra: The theoretical infrared spectra of the complexes (**I-IV**) with the free ligands, structures (1-7) are calculated by using Gaussian program [16] (B_3LYP, 6-31G) d,p) method (Tables 11-13) and compared with experimental data as follows:

• The theoretical calculations for complex **I** pointed to the symmetric and asymmetric stretching vibrations of CH taking place within the $\nu(C_3H_{10}H_{11})$ group are calculated at 3280 and 3332 cm^{-1}. However, the experimental values show two bands at 3101 and 3186 cm^{-1}. The $\nu(N_1\text{-}H_9)$ stretching vibration is calculated at 3663 cm^{-1}, while the experimental value is at 3558 cm^{-1}. The calculated $\nu(C_2\text{-}C_3)$ and $\nu(C_3\text{-}C_4)$ stretching vibrations are at 1673 cm^{-1} while the experimental value is at 1619 cm^{-1}.

• Also the $\nu(C_4\text{-}N_5)$ and $\nu(C_2\text{-}N_1)$ stretching vibration are calculated at 1511 cm^{-1} while the experimental value is at 1528 cm^{-1}. The calculated $\nu(O_{15}\text{-}H_{16})$ and $\nu(O_{15}\text{-}H_{17})$ stretching vibrations of OH in water molecules, 3877.57 cm^{-1}, far from the experimental value, 3186 cm^{-1}.

• For complex **II**, the $\nu(C_2\text{-}C_3)$ and $\nu(C_3\text{=}C_4)$ stretching vibrations are calculated at 1543 cm^{-1} while the experimental value is 1585 cm^{-1}. On the other hand the $\nu(C_6\text{=}N_5)$ and $\nu(C_6\text{-}N_1)$ stretching vibrations are calculated at 1449 cm^{-1} while the experimental value at 1473 cm^{-1}. The calculated $\nu(O_{15}\text{-}H_9)$, $\nu(O_{15}\text{-}H_{16})$, $\nu(O_{17}\text{-}H_{14})$ and $\nu(O_{17}\text{-}H_{14})$ stretching vibrations appear at 3725 cm^{-1} which is far from the experimental value, 3182 cm^{-1}.

• The theoretical infrared spectra of complex **III** are compared with experimental one as follows; the $\nu(C_3\text{-}H_{10})$ stretching vibration is calculated at 3022 cm^{-1} while the experimental value of this vibration is recorded at 3102 cm^{-1}. On the other hand the calculated $\nu(C_2\text{=}C_3)$ and $\nu(C_3\text{-}C_4)$ stretching vibration at 1582 cm^{-1} while the experimental value at 1572 cm^{-1}. Also The $\nu(C_6\text{=}N_1)$ and $\nu(C_6\text{-}N_5)$ stretching vibration are calculated at 1421 cm^{-1} while the experimental at 1438 cm^{-1}

• For complex **IV**, the calculated $\nu(C_2\text{-}C_3)$ and $\nu(C_3\text{=}C_4)$ stretching vibration are in the range of 1330-1507 cm^{-1} while the experimental value at 1562 cm^{-1}. The $\nu(C_4\text{-}H_{11})$ stretching vibration is calculated at 2932 cm^{-1} and the experimental value is recorded at 3083 cm^{-1}. From the above data, the theoretical calculations are compared with experimental spectra where more or less concordant results are obtained

Thermal analysis

TG and mechanism of decomposition: Thermogravimetric analysis (TGA) of the complexes are used to get information about thermal stability of these new complexes (Table-14). The thermal degradation of complex **I** started at 20 °C and ended at 600 °C. The first step of decomposition occurred in the range 50.87-117.73 °C (endothermic peak) with weight loss 13.053 % (calc. 13.42 %) corresponding to the loss of CH_3OH molecule. The second step occurred at the range 117.73-252.77 °C with weight loss 22.829 % (calc. 22.85 %) corresponding to the loss of H_2O and HCl molecules while

TABLE-12
THEORETICAL AND EXPERIMENTAL INFRARED SPECTRA OF THIOBARBITURIC ACID AND ITS COMPLEX

SBA			SBA·3NaCl		
Gaussian	Experimental	Assignment (cm^{-1})	Gaussian	Experimental	Assignment (cm^{-1})
3604	3563	$\nu(N_5\text{-}H_{9)}$, $\nu(N_1\text{-}H_8)$	3022	3102	$\nu(C_3\text{-}H_{10})$
3116	3104	$\nu(C_3\text{-}H_{12}\text{-}H_{13})$ asym.	1551	1717	$\nu(C_4\text{-}O_{11}^-)$, $\nu(C_2\text{-}O_9^-)$
3080	3104	$\nu(C_3\text{-}H_{12}\text{-}H_{13})$ sym.	1421	1438	$\nu(C_6\text{=}N_1)$, $\nu(C_6\text{-}N_5)$
1820	1693	$\nu(C_2\text{=}O_{10})$, $\nu(C_4\text{=}O_{11})$	1582	1572	$\nu(C_2\text{=}C_3)$, $\nu(C_3\text{-}C_4)$
1148	1163	$\nu(C_6\text{=}S_7)$			
1437	1442	$\nu(C_6\text{-}N_1)$, $\nu(C_6\text{-}N_{5)}$			

TABLE-13
THEORETICAL AND EXPERIMENTAL INFRARED SPECTRA OF THIOURACIL AND ITS COMPLEX

TU			TU·3KCl		
Gaussian	Experimental	Assignment (cm^{-1})	Gaussian	Experimental	Assignment (cm^{-1})
3642, 3608	3465	$\nu(N_5\text{-}H_{11})$, $\nu(N_1\text{-}H_{12)}$	2932	3083	$\nu(C_4\text{-}H_{11})$
3265, 3225	3084	$\nu(C_3\text{-}H_{10})$, $\nu(C_4\text{-}H_9)$	1330-1507	1562	$\nu(C_2\text{-}C_3)$, $\nu(C_3\text{=}C_4)$
1815	1706	$\nu(C_2\text{=}O_8)$	–	1421	$\nu(C_6\text{=}N_5)$, $\nu(C_6\text{-}N_1)$
1682	1625	$\nu(C_3\text{=}C_4)$	–	1165	$\nu(C_6\text{-}S_7^-)$
1407	1425	$\nu(C_6\text{-}N_1)$, $\nu(C_6\text{-}N_5)$	–	1702	$\nu(C_2\text{-}O_9^-)$
1163	1166	$\nu(C_6\text{-}S_7)$			

TABLE-14
THERMOGRAVIMETERIC (TGA) RESULTS OF THE COMPLEXES

Complex	Temp. (°C)	Loss found (%)	Loss calculated (%)	Assignment
I	50.87-117.73	13.053	13.42	CH_3OH
	117.73-252.77	22.829	22.85	H_2O + HCl
	337.95-507.78	64.118	64.15	COOH + C_2N_2 + KOH
II	22.14-503	24.608	25.406	H_2O + HCl + CO_2
	503-596.79	75.392	74.562	$C_3H_4N_2$ + 2Cl + K_2O + KOH
III	58.12-299.46	54.296	56.805	H_2O + H_2S + 3Cl + Na
	299.46-499.79	26.718	26.912	2C + Na_2O
	499.79-730.88	18.986	18.78	C_2N_2
IV	93.47-204.57	6.234	5.1187	H_2O
	204.57-399.77	85.507	85.77	HCl + 2Cl + N_2 + K_2O + KSH
	399.77-596.89	8.256	9.000	CH_3OH

the third step in the range 337.95-507.78 °C with weight loss 64.118 % (calc. 64.15 %) corresponding to the loss of COOH, C_2N_2 and KOH molecules. The DTA of this complex showed two endothermic peaks at (92.64 and 230.27 °C) and one exothermic peak at 419.23 °C.

For the TGA curve of complex **II**. The first step of decomposition occurred at the range 22.14-503 °C with weight loss 24.608 % (calc. 25.406 %) corresponding to the loss of H_2O, HCl and CO_2 molecules and the second step occured at the range 503-596.79 °C with weight loss 75.392 % (calc. 74.562 %) due to the loss of $C_3H_4N_2$, 2Cl, K_2O and KOH molecules. The DTA showed two exothermic peaks at (364.90 and 436.27 °C).

For the TGA curve of complex **III**, the first step of decomposition occurred in the range 58.12-299.46 °C with weight loss 54.296 % (calc. 56.805 %) corresponding to the loss of H_2O, H_2S, 3Cl and Na molecules while the second step at the range 299.46-499.79 °C with weight loss 26.718 % (calc. 26.912 %) due to the loss of 2C and Na_2O molecules. The DTA showed two exothermic peaks at (364.90 and 436.27 °C). The third step occured at the range 499.79-730.88 °C with weight loss 18.986 % (calc. 18.78 %) due to the loss of C_2N_2 molecule. The DTA of this complex showed three endothermic peaks at (80.08, 243.68 and 481.61 °C).

For the thermal decomposition of complex **IV**, the first step of decomposition occurred at the range 93.47-204.57 °C with loss 6.234 % (calc. 5.1187 %) of weight due to the loss of H_2O molecule. The second step occurred at the range 204.57-399.77 °C with weight loss 85.507 % (calc. 85.77 %) due to the loss of HCl, 2Cl, N_2, K_2O and KSH molecules, while the third step occured at the range 399.77-596.89 °C with weight loss 8.256 % (calc. 9.00 %) due to the loss of CH_3OH molecule. The DTA showed two endothermic peaks at (290.08 and 504.18 °C).

Differential thermal analysis: Fig. 3 shows plots of ln ΔT *versus* 1/T for the complexes, for each DTA curve, gave straight lines from which the activation energies (E_o) are calculated. The thermodynamic parameters of decomposition processes of compounds, namely enthalpy ΔH and entropy ΔS are evaluated [30-35]. The order of chemical reaction is calculated *via* peak symmetry method [36].

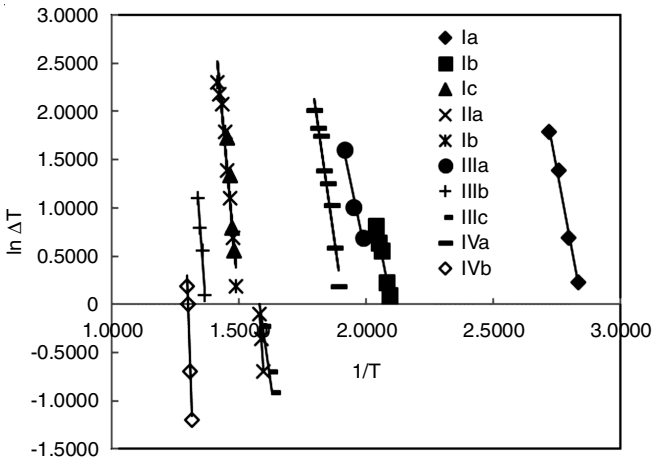

Fig. 3. ln DT-1/T relation for complexes (**I-IV**)

The values of the change of entropy ΔS for all complexes (Table-15), are of the same magnitude within the range of (-0.299 to -0.023) kJ K^{-1} mol^{-1}. The values of the decomposed substance fraction α are in the range (0.54-0.68). The change

TABLE-15
THERMAL ANALYSIS DATA OF THE COMPLEXES

Complex	Type	Slope	E_a (kJ mol^{-1})	n	α	T_m (K)	Z (s^{-1})	ΔS (kJ/mol K)	ΔH (kJ mol^{-1})
I	Endo	-14005	116.44	1.15	0.606	365.6	115.63	- 0.207	113.40
	Endo	-13129	109.15	1.63	0.54	503.3	74.68	- 0.213	104.96
	Exo	- 48950	406.97	1.46	0.561	692.2	71.81	- 0.039	401.215
II	Exo	-39507	328.46	1.782	0.522	637.9	63.03	- 0.215	323.16
	Exo	-31960	265.71	1.26	0.589	709.3	46.12	- 0.023	259.81
III	Endo	-12580	104.59	0.891	0.653	516.7	25.39	- 0.033	100.29
	Endo	-17771	147.75	1.18	0.602	641.5	28.74	-0.223	142.42
	Endo	-35876	298.27	0.753	0.683	754.6	48.60	-0.220	291.99
IV	Endo	-18716	155.60	1.173	0.602	563.1	95.83	-0.212	150.92
	Endo	-69652	579.09	0.760	0.681	777.2	273.38	-0.299	572.63

of enthalpy, ΔH values for any peak temperature T_m can be given by the following equation $\Delta S = \Delta H/T_m$ are with + ve signs, where processes are endothermic.

The DTA data gave the following: (i) first order kinetics (ii) negative values of entropy for all complexes where the transition states are more ordered thus in a less random molecular configuration than reactants.

Differential scanning calorimetry: Differential scanning calorimetry (DSC) is used to measure the excess heat capacity (Cp) of the sample solution with respect to the reference (usually aqueous) solvent. The DSC curves are obtained for barbituric, thiobarbituric, thiouracil and their complexes which done under a flow of N_2 at heating rate 10 °C/min in the temperature range 300-650 °C.

The Debye model [17] is applied to describe the change of heat capacity with temperature range as empirical equation:

$$Cp = a\,T + b \qquad (13)$$

Fig. 4 shows full Cp-T while Cp-T relation for the straight line is represented by (B) for complex (**III**) as example. From the slopes and the intercepts of Cp-T relations, a and b can be calculated (Table-16). Another application of Debye model on investigated complexes by the following equations:

$$Cp = \alpha T^3 + \gamma T,\ Cp/T = \alpha T^2 + \gamma \qquad (14)$$

where α and γ are the coefficients of electronic and lattice heat capacities respectively, Fig. 5 shows plots of (Cp/T) *versus* T^2 for complex (**III**). The full relation (Cp/T) *versus* T^2, similarly $(C_P/T) - T^2$ relation analyzed in similar way to (B) should yield straight lines with slope α and intercept γ (Table-17). The straight lines are analyzed (figure not shown) and their reasonable equations are given with higher R^2 values for each line.

Evaluation of kinetic parameters: The following equation is applied [34-37]:

$$\ln [-\ln (1-\alpha)/T^2] = (-E_a/RT) + \ln AR/\beta E_a \qquad (15)$$

Plot of left hand side *versus* 1/T, from the above equation (figure not shown) is found to be linear where E_a is calculated from the slope and A is calculated from the intercept. The enthalpy (ΔH) is calculated from the following equation, $\Delta H = E_a - RT$. The entropy of activation ΔS ($J\,K^{-1}$) is calculated from:

$$\Delta S = R \ln (A\,h/K\,T_S)$$

where K is the Boltzmann constant, h is the Plank's constant and T_s is the DTG peak temperature. ΔG is calculated from $\Delta G = \Delta H - T\Delta S$ (Table-18).

The E_a values for the investigated complexes (**I-IV**) are evaluated [37-40].

$$\ln\ln (1-\alpha)^{-1} = (E_a/RT^2_s)\theta \qquad (16)$$

$\ln\ln (1-\alpha)^{-1}$ *versus* θ plots exhibit straight lines (figure not shown). Thermodynamic parameters of investigated complexes (**I-IV**) are calculated and shown in Table-18. All decomposition

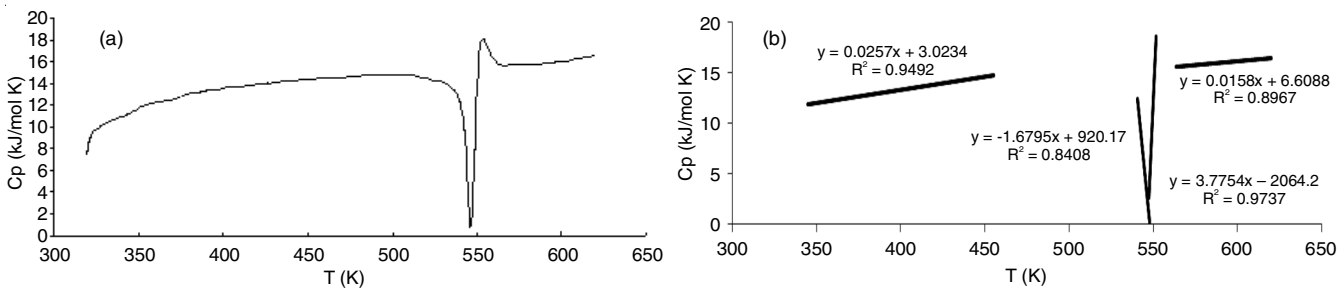

Fig. 4. CP-T relation for complex **III** (SBA.3NaCl)

TABLE-16
THE SLOPES 'a' AND INTERCEPTS 'b' FOR DSC CURVES OF COMPLEXES (Cp = a T + b)

Complex	a_1 (b_1)	a_2 (b_2)	a_3 (b_3)	a_4 (b_4)	a_5 (b_5)	a_6 (b_6)	a_7 (b_7)
$BA.KCl.2H_2O$	0.1235	-0.3959	1.1718	0.0154	-0.2454	0.9277	0.0263
(**I**)	(-27.053)	(145.15)	(-434.92)	(8.2299)	(133.39)	(-458.85)	(1.6372)
$BA.3KCl.2H_2O$	0.4409	0.1008	0.3118	0.036	0.0267	-0.0241	–
(**II**)	(-124.21)	(43.466)	(-102.13)	(0.6466)	(3.5896)	(32.995)	
SBA.3NaCl	0.0257	-1.5274	3.7754	0.0155	–	–	–
(**III**)	(3.0234)	(837.7)	(-2064.2)	(6.7891)			
TU.3KCl	-0.0181	-0.225	0.298	-0.0237	–	–	–
(**IV**)	(23.31)	(111.71)	(-134.99)	(24.959)			

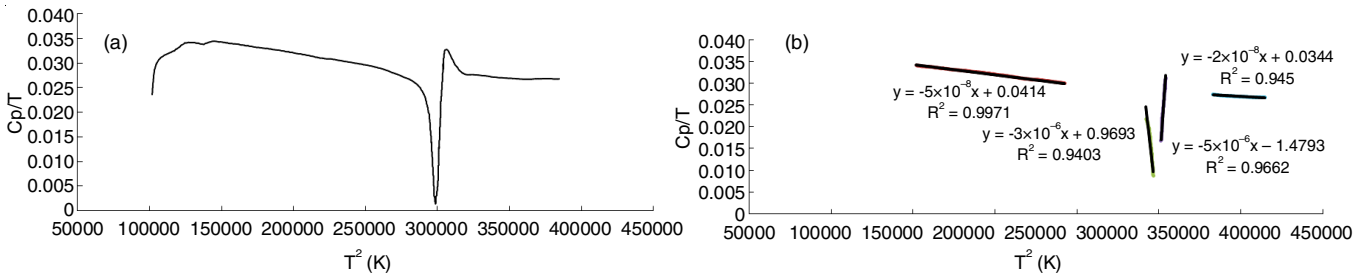

Fig. 5. CP/(T-T^2) relation for complex **III** (SBA.3NaCl)

TABLE-17
THE SLOPES (α) AND INTERCEPTS (γ) FOR DSC CURVES OF COMPLEXES ($Cp/T = \alpha T^2 + \gamma$)

Complex	α_1 (γ_1)	α_2 (γ_2)	α_3 (γ_3)	α_4 (γ_4)	α_5 (γ_5)	α_6 (γ_6)	α_7 (γ_7)	α_8 (γ_8)
BA.KCl.2H_2O	8×10^{-7}	-2×10^{-6}	4×10^{-6}	-6×10^{-8}	-8×10^{-7}	2×10^{-6}	-3×10^{-8}	-2×10^{-8}
(**I**)	(0.0374)	(0.2138)	(-0.6011)	(0.0459)	(0.2137)	(-0.3909)	(0.0386)	(0.0381)
BA.3KCl.2H_2O	3×10^{-6}	-7×10^{-7}	8×10^{-7}	-6×10^{-8}	-5×10^{-8}	–	–	–
(**II**)	(-0.2723)	(0.1035)	(-0.0768)	(0.0497)	(0.047)			
SBA.3NaCl	-5×10^{-8}	-3×10^{-6}	5×10^{-6}	-2×10^{-8}	–	–	–	–
(**III**)	(0.0414)	(0.9693)	(-1.4793)	(0.0344)				
TU.3KCl	-3×10^{-7}	-5×10^{-7}	6×10^{-7}	-6×10^{-8}	–	–	–	–
(**IV**)	(0.0908)	(0.123)	(-0.1216)	(0.0398)				

TABLE-18
THERMODYNAMIC PARAMETERS EVALUATED BY COATS-REDFERN AND HOROWITZ METZGER EQUATIONS (15,16)

Complex	Coats-Redfern				Horowitz Metzger			
	E_a (kJ)	ΔS (J/mol K)	ΔH (kJ/mol)	ΔG (kJ/mol)	E_a (kJ)	ΔS (J/mol K)	ΔH (kJ/mol)	ΔG (kJ/mol)
BA·KCl·2H_2O (**I**)	142.4438	-54.15	136.9908	172.5067	143.0602	-21.846	137.6072	151.9163
BA·3KCl·2H_2O (**II**)	121.4925	-87.466	115.5727	176.8989	109.994	-105.75	104.174	178.199
SBA·3NaCl (**III**)	109.221	-46.094	104.9169	128.7797	124.782	-13.282	120.478	127.356
TU·3KCl (**IV**)	168.0758	41.910	163.3867	139.7495	196.266	94.06	191.577	138.527

stages show that the best fit for n = 1, the negative values of entropy of activation indicate the fragments have ordered structures than undecomposed complexes. The positive values of enthalpy of activation of the decomposition stages indicate that the process is endothermic. The positive values of free energy of the decomposition indicate that non-spontaneous process.

The plot of ΔH *versus* ΔS for the complexes **I**, **II** and **IV** are linear (r = 0.975) for both methods (figure not shown). The isokinetic temperature β is 407 K, which is lower than experimental temperature range, confirming the processes is entropy control. However, such plots for the complexes under investigation in both methods lie on the same straight line indicating a close similarity in the mechanism for complexes **I, II, IV** but for **III** with different mechanism.

CONFLICT OF INTEREST

The authors declare that there is no conflict of interests regarding the publication of this article.

REFERENCES

1. N.Z. Shaban, M.S. Masoud, M.A. Mawlawi, D. Awad and O.M. Sadek, *J. Physiol. Biochem.*, **68**, 475 (2012); https://doi.org/10.1007/s13105-012-0160-4.
2. R.Y. Levina and F.K. Velichko, *USP Khim. Russ. Chem. Rev.*, **29**, 929 (1960).
3. M. Holtkamp and H. Meierkord, *Cell. Mol. Life Sci.*, **64**, 2023 (2007); https://doi.org/10.1007/s00018-007-7021-2.
4. M. Kidwai, R. Thakur and R. Mohan, *Acta Chim. Slov.*, **52**, 88 (2005).
5. D.R. Janero, *Free Radic. Biol. Med.*, **9**, 515 (1990); https://doi.org/10.1016/0891-5849(90)90131-2.
6. P.Y. Shirodkar and M.M. Vartak, *Indian J. Heterocycl. Chem.*, **9**, 239 (2000).
7. W.G. Brouwer, E.E. Felauerand and A.R. Bell, U.S. Patent, 779982 (1990); *Chem Abstr.*, **114**, 185539 (1991).
8. B.B. Semenov, I.I. Levina and K.A. Krasnov, *Pharm. Chem. J.*, **39**, 29 (2005); https://doi.org/10.1007/s11094-005-0073-4.
9. Archana, V.K. Srivastava and A. Kumar, *Bioorg. Med. Chem.*, **12**, 1257 (2004); https://doi.org/10.1016/j.bmc.2003.08.035.
10. A. Nagasaka and H. Hidaka, *J. Clin. Endocr. Metab.*, **43**, 152 (1976); https://doi.org/10.1210/jcem-43-1-152.
11. S. Shigeta, S. Mori, T. Kira, K. Takahashi, E. Kodama, K. Konno, T. Nagata, H. Kato, T. Wakayama, N. Koike and M. Saneyoshi, *Antivir. Chem. Chemother.*, **10**, 195 (1999); https://doi.org/10.1177/095632029901000404.
12. M. Bretner, T. Kulikowski, J.M. Dzik, M. Balinska, W. Rode and D. Shugar, *J. Med. Chem.*, **36**, 3611 (1993); https://doi.org/10.1021/jm00075a016.
13. T. Wandlowski and M.H. Holzle, *Langmuir*, **12**, 6604 (1996); https://doi.org/10.1021/la9607619.
14. W. Li, W. Haiss, S. Floate and R.J. Nichols, *Langmuir*, **15**, 4875 (1999); https://doi.org/10.1021/la9815594.
15. X. Zhai and S. Efrima, *Phys. Chem.*, **100**, 1779 (1996); https://doi.org/10.1021/jp951901a.
16. M.J. Frisch, G.W. Trucks, H.B. Schlegel, G.E. Scuseria, M.A. Robb, J. R. Cheeseman, J.A. Montgomery Jr., T. Vreven, K.N. Kudin, J.C. Burant, J.M. Millam, S.S. Iyengar, J. Tomasi, V. Barone, B. Mennucci, M. Cossi, G. Scalmani, N. Rega, G.A. Petersson, H. Nakatsuji, M. Hada, M. Ehara, K. Toyota, R. Fukuda, J. Hasegawa, M. Ishida, T. Nakajima, Y. Honda, O. Kitao, H. Nakai, M. Klene, X. Li. J.E. Knox, H.P. Hratchian, J.B. Cross, V. Bakken, C. Adamo, J. Jaramillo, R. Gomperts, R.E. Stratmann, O. Yazyev, A.J. Austin, R. Cammi, C. Pomelli, J.W. Ochterski, P.Y. Ayala, K. Morokuma, G.A. Voth, P. Salvador, J.J. Dannenberg, V.G. Zakrzewski, S. Dapprich, A.D. Daniels, M.C. Strain, O. Farkas, D.K. Malick. A.D. Rabuck, K. Raghavachari, J.B. Foresman, J.V. Ortiz, Q. Cui, A.G. Baboul, S. Clifford, J. Cioslowski, B.B. Stefanov, G. Liu, A. Liashenko, P. Piskorz, I. Komaromi, R.L. Martin, D.J. Fox, T. Keith, M.A. Al-Laham, A. Nanayakkara, C.Y. Peng, M. Challacombe, P.M.W. Gill, B. Johnson, W. Chen, M.W. Wong, C. Gonzalez and J.A. Pople, Gaussian 03, Revision E.01, Gaussian, Inc.: Wallingford CT (2004).
17. J.M. Parmar and N.K. Joshi, *Int. J. Chemtech Res.*, **4**, 834 (2012).
18. M.S. Masoud, E.A. Khalil, A.M. Hindawy, A.E. Ali and E.F. Mohamed, *Spectrochim. Acta A*, **60**, 2807 (2004); https://doi.org/10.1016/j.saa.2004.01.019.
19. M.S. Masoud, S.A. Abou El-Enein and N.A. Obeid, *Z. Phys. Chem.*, **215**, 867 (2001).
20. J. Lorentzon, M.P. Fuelscher and B.O. Roos, *J. Am. Chem. Soc.*, **117**, 9265 (1995); https://doi.org/10.1021/ja00141a019.
21. M.S. Masoud and E.A. Khalil, *Pol. J. Chem.*, **65**, 933 (1991).
22. M.S. Masoud, A.K. Ghonaim and A.A. Mahmoud, 36th Annual Eastern. Analytical Symposium and Exposition, Somerset: New Jersey, USA, p. 525 (1997).
23. G. Miessler and D.A. Tarr, Inorganic Chemistry, Pearson Education Inc.: New Jersey (2004).
24. M.S. Masoud, A.A. Abdullah and F.N. Khairy, *The Indian Textile J.*, 103 (1983).

25. M.S. Masoud, M.A. El-Dessouky, F. Aly and S.A. Abu El-Enein, 2nd Chemistry Conference of Science, Alexendira University, **178**, 196 (1988).
26. M.A. Shaker and M.A. Khalifa, *Alex. J. Pharm. Sci.*, **9**, 159 (1995).
27. M.S. Masoud, A.E. Ali, M.A. Shaker and M.A. Ghani, *Spectrochim. Acta A Mol. Biomol. Spectrosc.*, **60**, 3155 (2004); https://doi.org/10.1016/j.saa.2004.02.030.
28. J.G. David and H.E. Hallam, *Spectrochim. Acta A Mol. Spectrosc.*, **23**, 593 (1967); https://doi.org/10.1016/0584-8539(67)80316-7.
29. M.S. Masoud, *J. Chem. Pharm. Res.*, **9**, 171 (2017).
30. R.W. Taft and M.J. Kamlet, *J. Am. Chem. Soc.*, **98**, 2886 (1976); https://doi.org/10.1021/ja00426a036.
31. M.S. Masoud, S.S. Haggag, H.M. El-Nahas and N.A. El-Hi, *Acta Chim. Hung.*, **130**, 783 (1993).
32. C. Rerchordt and T. Wetton, Solvents and Solvent Effects in Organic Chemistry, Wiley-VCH: Weinheim, edn 2 (2010).
33. M.S. Masoud, A. El-Merghany, A.M. Ramadan and M.Y. Abd El-Kaway, *J. Therm. Anal. Calorim.*, **101**, 839 (2010); https://doi.org/10.1007/s10973-010-0722-z.
34. M.S. Masoud, D.A. Ghareeb and S.S. Ahmed, *J. Mol. Struct.*, **1137**, 634 (2017); https://doi.org/10.1016/j.molstruc.2017.01.086.
35. H.H. Horowitz and G. Metzger, *Anal. Chem.*, **35**, 1464 (1963); https://doi.org/10.1021/ac60203a013.
36. H.L. Kissinger, *Anal. Chem.*, **29**, 1702 (1957); https://doi.org/10.1021/ac60131a045.
37. C. Degueldre, P. Tissot, H. Lartigue and M. Pouchon, *Thermochim. Acta*, **403**, 267 (2003); https://doi.org/10.1016/S0040-6031(03)00060-1.
38. A.R. Reddy and K.H. Reddy, *J. Appl. Polym. Sci.*, **92**, 1501 (2004); https://doi.org/10.1002/app.20076.
39. M.A. Ashok and B.N. Achar, *Bull. Mater. Sci.*, **31**, 29 (2008); https://doi.org/10.1007/s12034-008-0006-4.
40. S. Gopalakrishnan and R. Sujatha, *Der Chemica Sinica*, **2**, 103 (2011).